

Quench dynamics of two component dipolar Fermions in a Quasiperiodic potential

Bradraj Pandey⁽¹⁾, and Swapan K. Pati^(1,2)

⁽¹⁾ *LPTMS, CNRS, Univ. Paris-Sud, Université Paris-Saclay, 91405 Orsay, France*

⁽²⁾ *Theoretical Sciences Unit, Jawaharlal Nehru Centre for Advanced Scientific Research, Jakkur Campus, Bangalore 560064, India*

(Dated: June 16, 2022)

Motivated by the recent experiments in fermionic polar gases, we study quench dynamics of two component dipolar fermions, in presence and absence of quasiperiodic potential. We investigate the localization of charge and spin degree of freedom separately, by probing the local and global dynamical observables. In order to study non-equilibrium dynamics, we start with two different product states, doublons ($|\uparrow\downarrow 0 \uparrow\downarrow 0 \uparrow\downarrow 0 \uparrow\downarrow 0 \uparrow\downarrow \dots\rangle$) and a Neel state ($|\uparrow, \downarrow, \uparrow, \downarrow, \uparrow, \downarrow, \uparrow, \downarrow, \dots\rangle$). We carried out real long time dynamics of the fermionic Hamiltonian using exact-diagonalization and matrix-product-state formalisms. In case of doublons, we demonstrate the transition from delocalize to localize MBL phase, in presence of strong interactions and disorder. In case of Neel state, by taking strong enough disorder, we show the localization of spin degree of freedom is also possible along with the charge degree of freedom, when onsite and long-range interaction strength are equal in strength, without breaking the spin SU(2) symmetry of system Hamiltonian. Our predictions for localizations of both charge and spin degrees of freedom should be observed in experiment with fermionic dipolar atom subject to quasiperiodic potential.

PACS numbers: 03.75.Lm, 05.30.Jp, 05.30.Rt

I. INTRODUCTION

Recent advancement in ultra-cold atomic gases provides promising platform for studying non-equilibrium dynamics of interacting quantum systems^{1,2}. The perfect isolation from environment, and tunability of ultra-cold atomic gases, allow us to probe the unitary time evolution of isolated quantum systems³. The isolated system can go through thermalization process, where it loses the memory of the initial state, due to its own dynamics⁴⁻⁶. The system itself acts as a heat bath, in which exchange of energy and particle occurs⁷. However, integrable and localized systems fail to thermalize, preserving the memory of initial states^{8,9}. Recently, localized many body system with disorder potential has attracted huge interest due to its possible applications in quantum information theory and exploring of the new paradigms of statistical mechanics¹⁰.

Localization of non-interacting particles (Anderson localization (AL)) in presence of quenched disorder was first described by Anderson⁹, where the system shows absence of transport and thermalization. In low dimensional disordered system, the presence of interactions give rise to a many-body localization phase (MBL)¹¹⁻¹⁴. In fact, the many body localized phase shows very different characteristics in terms of spectral and dynamical properties in comparison to the ergodic systems¹⁵. In presence of sufficiently strong disorder, many-body localization occurs in full energy-spectrum, leads to area-law scaling of excited eigenstates¹⁶ (whereas ergodic system exhibit volume law scaling) and can be described by complete set of quasi-local integral of motion (LIOM)^{17,18}. In case of many-body localization, the energy level-spacing statistics follow Poisson distribution, whereas ergodic system follow Wigner-Dyson distribution¹³. The most popu-

lar way to characterize the MBL-phase, is to follow the real-time dynamics of some initial product state in presence of disorder and interactions. In MBL-phase, local-observable shows slow power-law decay with time and carry the memory of initial state^{19,20}. Interestingly, the transport of energy, charge and spins are prohibited in AL and MBL-phase, while in ergodic phase, one observes fast transfer energy and particles after sudden-quench²¹. The dynamics of entanglement entropy provides an important tool to differentiate between AL, MBL and thermal phases. For short range interacting disordered system, in the MBL phase, the entanglement entropy increases logarithmically with time^{22,23}, in the AL phase entanglement entropy saturate to a small finite value after a short time, whereas, in ergodic phase entanglement grows ballistically with time²¹.

Recent experiments in cold atomic systems in presence of disorder or quasi-periodic potential, substantiate the theoretical and numerical predictions of MBL-phase quite well²⁴⁻²⁷. In Ref²⁴, the many-body localization of interacting fermionic system in quasiperiodic potential has been shown, by observing the decay of density imbalance with time. The system has been modeled in terms of Fermionic Hubbard model and the time evolution has been carried out with charge density states. Recently, by the same group with similar experimental setup, the observation of slow dynamics near the MBL-phase transition has been demonstrated²⁶. In another experiment²⁷, working with long-range interaction spin system (initialize with a Neel state) in presence of random transverse field, observation of long-term memory of local-magnetization, poissonian distribution of level statistics and growth of entanglement entropy has been observed.

Interestingly, most of the experiments have been performed with spinfull fermionic Hubbard model, where

system has continuous non-Abelian $SU(2)$ symmetry. It has been suggested that, in presence of non-Abelian symmetry system can not have full-MBL phase even at large disorder^{28–30}. The fermions have charge and spin, both local degrees of freedom and in presence of disorder they can show different localization behavior. Numerical study of one-dimensional disorder Hubbard model (disorder in charge sector) shows that charge degree of freedom localized while spin degree of freedom is delocalized³¹. Furthermore, in Ref³², using t-DMRG on fermionic Hubbard model with disorder, authors conclude that after long time spin dynamics become non-ergodic and entanglement grow logarithmically. In Ref³³, by mapping the Hubbard model to an effective spin Heisenberg model in presence of large disorder, sub-diffusive transport of spin has been observed. The restoration of full MBL phase has been demonstrated in Ref³⁴, by breaking the spin $SU(2)$ (using asymmetrical spin hopping), which leads to localization of spin also. The presence or absence of full-body localization in $SU(2)$ symmetry systems is an ongoing topic of research. In most recent study³⁵, it has been argued that, delocalization of spin can also lead to delocalization of charge after very long time, depending upon the occupancy of fermions.

Motivated by recent experimental progress in polar Fermi gases^{36,37}, and experiments on MBL-phase with fermionic systems^{24,26}, we study the localization of charge and spin degree of freedom, in presence of long range dipolar interactions with quasiperiodic on-site potential. To probe localization, we follow the sudden quench protocol, starting with two simple and experimentally accessible initial product states, a charge density state ($|\uparrow\downarrow 0 \uparrow\downarrow 0 \uparrow\downarrow 0 \uparrow\downarrow 0 \uparrow\downarrow \dots\rangle$) and a Neel state ($|\uparrow, \downarrow, \uparrow, \downarrow, \uparrow, \downarrow, \uparrow, \downarrow, \uparrow, \downarrow, \dots\rangle$). By analyzing the dynamics of local observable like density and spin imbalance and also global observable like entanglement, charge and spin fluctuations, with different interaction parameters and disorder strength, we are able to show the localization of spin and charge separately. First we explore the non-equilibrium dynamics with product state without any disorder, to trace the region of localization or delocalization for different interactions parameters. Then we demonstrate the transition from delocalize to localize MBL-phase, for product state with doublons subject to quasiperiodic potential. Most prior works with long-range interaction have focused on localization of charge sector (spinless fermions). Here, we study the effect of long-range interaction on spin degree of freedom, with large disorder strength, where charge degree of freedom already localizes. Furthermore, by calculating spin-auto correlation function for each eigen-states of system Hamiltonian, we demonstrate localization of spin degree of freedom in full energy spectrum.

The remaining part of the article is organized as follows: In Sec. II, we have discuss the model Hamiltonian and the method used. Section III has the results and discussion part and it is divided into two subsections A and B. In subsection A, we discuss non-equilibrium dynamics

for product states with doublons and Neel state without disorder. While in subsection B, we show localization of spin and charge in presence of quasiperiodic potential. In Appendix, we provide intuitive description of localization of spin-degree of freedom, in presence of large disorder. We have checked our results with matrix product state calculation for larger system sizes³⁸.

II. MODEL AND METHOD

We consider two-component (pseudo-spin-1/2) dipolar Fermions in a 1D lattice at half-filling. The effective Hamiltonian of the system can be written as,

$$H = J \sum_{\sigma,i} \left(c_{\sigma,i}^\dagger c_{\sigma,i+1} + h.c \right) + U \sum_i \hat{n}_{i,\uparrow} \hat{n}_{i,\downarrow} + \sum_{(i \neq j)} V(i,j) \tilde{n}_i \tilde{n}_j + \Delta \sum_{i,\sigma} \hat{n}_i \cos(2\pi\beta i + \phi) \quad (1)$$

where $c_{\sigma,i}$ is the annihilation operator with spin $\sigma = \uparrow, \downarrow$ at site i . Here \uparrow and \downarrow states refer to two hyperfine states of dipolar atoms or molecules. $\tilde{n} = (\hat{n} - \langle n \rangle)$ where \hat{n} is the number operator and $\langle n \rangle$ is the average number in each site, which is taken as 1, as it is half filled system. J is the hopping term and U is the onsite interaction term; $V(i,j)$ is the long range interaction term, which depend on diction and distance between the polarize dipoles as $V_{dd} \propto (1 - 3\cos(\theta)^2)/r^3$. In an optical lattice by using feshbach resonance or by changing the lattice depth, one can modulate the onsite-interaction U . The model in Eq.1, preserves $U(1)$ and $SU(2)$ symmetries, related to conservation of total particle number, N , and total spin of the system. At half filling, when V and Δ are zero, the system has a particle-hole symmetry on one of the spin components ($c_{j,\downarrow} \rightarrow (-1)^j c_{j,\downarrow}^\dagger$). This mapping provides a hidden charge $SU(2)$ symmetry in addition to the spin $SU(2)$ symmetry, which results in $SO(4)$ symmetry in total³⁹. On the other hand, in presence of V , the charge $SU(2)$ symmetry reduced to $U(1)$, while spin $SU(2)$ symmetry unaffected^{40,41}. To study the effect of strong interactions on localization of spin and charge degree of freedom in presence of disorder, we have added quasi-periodic onsite potential^{42,43}. The strength of disorder is measured by the coefficient, Δ , of the quasiperiodic potential and we choose $\beta = (\sqrt{5} - 1)/2$.

In order to study the non-equilibrium dynamics, we initialize the system in a charge density wave with doublons (for localization of charge), and a Neel state (mainly for localization of spin). These product states correspond to highly excited states in the energy spectrum of system Hamiltonian. In case of Neel state, for the interaction parameters we studied, the expectation values ($\langle \Psi_i | H | \Psi_i \rangle$) corresponding to Eq.1, almost belong to the middle part of the energy spectrum (equivalent to an infinite temperature state). We have investigated the time evolution of these initial states ($|\Psi(0)\rangle$), in the influence of the Hamiltonian, as $\Psi(t) = \exp(-iHt)|\psi(0)\rangle$. In this article, we

have studied the problem numerically; we have used time dependent exact-diagonalization (ED) method (for system size $L = 8, 10$ and 12), also Matrix Product States (MPS) calculations for $L = 24$ (which is given in Appendix). For precise convergence of the wave-function, the time step δt has been considered to be very small (0.005 in units of \hbar/J for ED and 0.0001 for MPS).

III. RESULTS AND DISCUSSION

A. Clean system without disorder

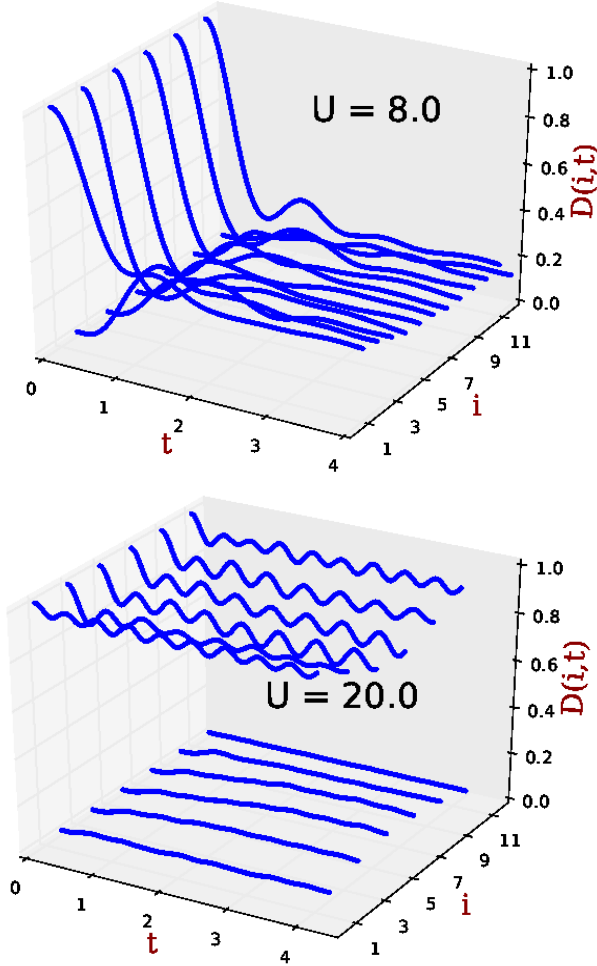


FIG. 1. Time evolution of local double occupancy $D(i, t)$, with sites and time, t (in units of \hbar/J), for $U = 8$ and $U = 20$ at $V = 8$, $L = 12$.

In this subsection, we investigate the dynamics of products states in the absence of disorder. First we study the localization of charge and spin degree of freedom with system initialize in a product state with doublons $|\uparrow\downarrow 0 \uparrow\downarrow 0 \uparrow\downarrow 0 \uparrow\downarrow 0 \uparrow\downarrow \dots\rangle$ for $V = 4$, $\Delta = 0$ and different values of onsite interaction U . Fig.1 shows the time evolution of the local double occupancy defined as

$D(i, t) = \langle n_{i\uparrow} n_{i\downarrow} \rangle$, at $V = 4$ and for two different values of onsite interactions $U = 8$ (near the critical point of CWD to SDW transition⁴⁴ of the Hamiltonian for $\Delta = 0$) and $U = 20$ (far away from critical point). We find for $U = 8$, doubly occupied sites decay quickly ($t \sim \hbar/J$) to a small finite value, and after few oscillations each sites have approximately same small doublon occupancy. On the otherhand, for $U = 20$ the number of doublons almost retain the same initial value. At $U \sim 2V$ doublons are unstable and can decay to two individual fermions, as the energy requires for two fermions to occupy the nearest-neighbor sites approximately the same as two fermions residing on the same site⁴⁵. Although the total number of doublons takes some finite values (Fig.1(a)), it suggests that system can be describe by linear combination of individual fermions resides on adjacent sites with doubly occupied sites⁴⁵. While away from critical value doublons are quite stable and can hops slowly through second order process.

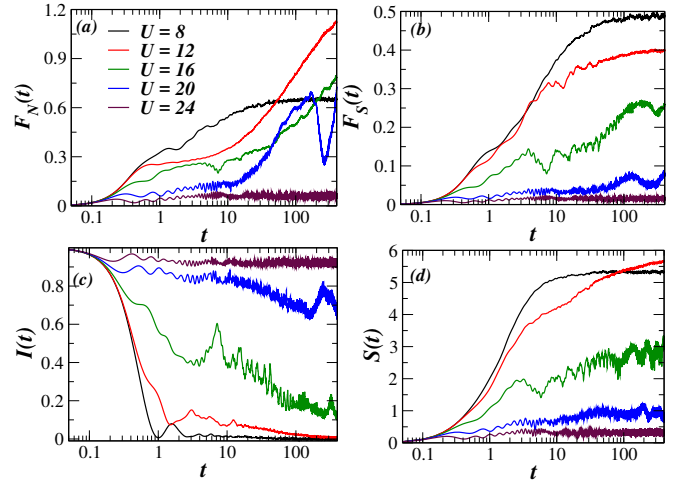


FIG. 2. (a) Bipartite charge-fluctuation $F_N(t)$, (b) bipartite spin-fluctuation $F_S(t)$ (c) charge imbalance $I(t)$, (d) entanglement entropy $S(t)$, with time t (in units of \hbar/J), at $V = 4$ and different values of U

To explore the transport of charge and spin in the system⁴⁶, for the initial CDW state with time, we have calculated time dependent bipartite fluctuations of charge (\hat{N}) and z-component of spin (\hat{S}^z). The system ($L = 12$) can be divided in to two part: block A and B, the charge fluctuations of block A, can be defined as⁴⁷ $F_N(t) = \langle \Psi(t) | N_A^2 | \Psi(t) \rangle - \langle \Psi(t) | N_A | \Psi(t) \rangle^2$, where $N_A = \sum_{i=1}^{L/2} \hat{n}_i$. Similarly, the z-component of spin fluctuation of block A can be defined as, $F_S(t) = \langle \Psi(t) | (S_A^z)^2 | \Psi(t) \rangle - \langle \Psi(t) | S_A^z | \Psi(t) \rangle^2$, where $S_A^z = \sum_{i=1}^{L/2} s_i^z$. These charge and spin fluctuations can be related to transport of charges and z-component of spins from block A to B^{46,48}. As shown in Fig.2, the charge and spin fluctuations occurs maximally around $U \sim 2V$, while for large U , $F_N(t)$ and $F_S(t)$ saturates to a small value after a short time. As explained previously, near the critical region $U \sim 2V$, doublons dissociate into single particle maximally, which re-

sults in maximum charge and spin fluctuations for $U = 8$. On the other hand for $U > 2V$, doublons are quite stable and hops very slow through second order process, which leads to decrease in charge and spin fluctuations in the system. For moderate values of U , charge and spin fluctuation shows different behavior. Interestingly, for these values of U , doublons can hop without breaking into single fermions, which leads to more charge fluctuations $F_s(t)$ compare to spin fluctuations $F_s(t)$.

To measure the extent of localization of CDW product state without disorder, we have calculated the charge imbalance²⁴ $I(t) = \frac{N_e - N_o}{N_e + N_o}$, where N_e and N_o are the sum of numbers of atoms on even and odd sites respectively. As shown in Fig.2(c), for $U = 8$, imbalance $I(t)$ quickly relax to zero, indicating delocalization of the initial states. For moderate values of U , initial states decays algebraically and after long time it tends toward zero. Furthermore, for large values of U , imbalance $I(t)$ almost retain the same values of the initial state, indicating localization of the system. In Fig.2(d), we have calculated the Von Neumann entropy of subsystem A (dividing the system $L = 10$ in two equal blocks A and B), $S(t) = -\text{Tr} \rho_A(t) \ln \rho_A(t)$, where $\rho_A(t)$ is the reduced density matrix of A at time t . As can be seen, near the critical region, the entanglement entropy, $S(t)$ grows rapidly with time t , indicating the strong delocalization in the system. On the otherhand for large U , entanglement entropy $S(t)$, increases quite slowly or reach to a small constant value, indicate localization of the initial CDW state. The very slow increase of entanglement with time also due to the fact that for larger values of U , the initial product state with doublons very close to being an eigenstate of the system Hamiltonian⁴⁹.

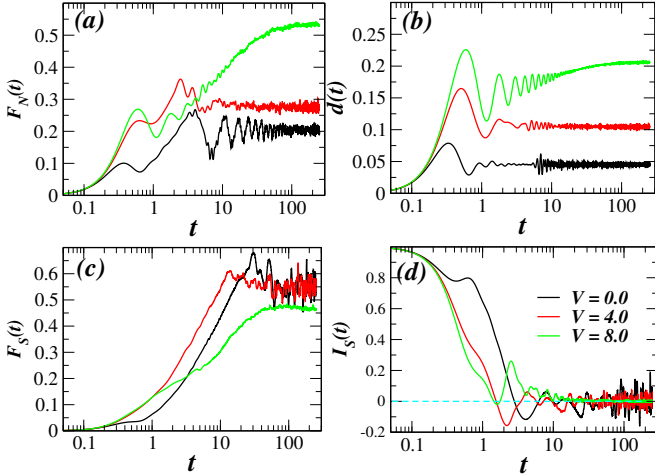


FIG. 3. (a) Bipartite charge-fluctuation $F_N(t)$, (b) Average double occupancy $d(t)$ (c) bipartite spin-fluctuation $F_S(t)$, (d) spin imbalance $I_S(t)$, with time t (in units of \hbar/J), at $U = 8$, $L = 12$ and different values of V

Next, we study the decay of a Neel state $|\uparrow, \downarrow, \uparrow, \downarrow, \uparrow, \downarrow, \uparrow, \downarrow, \dots\rangle$, for onsite interaction $U = 8$, $\Delta = 0$ and different values of long-range interaction V . The

case of $V = 0$ with different U , has been studied in Ref⁵⁰, where they found that, short term dynamics controlled by charge-excitations, while longer time dynamics of the system by spin-excitations. The spin excitations can move in the system by exchange mechanism ($\sim 4J^2/U$). As shown in Fig.3(d), for $V = 0$ the total staggered magnetization or spin imbalance^{51,52}, $I_S(t) = \frac{2}{L} \sum_i (-1)^{i+1} s_i^z(t)$, decay fast and oscillate around zero, while spin fluctuations $F_S(t)$, increase rapidly and after a short time, oscillate around a fixed values. On the otherhand introduction of long-range interaction V , leads to enhancement in charge fluctuations $F_N(t)$ (Fig.3(a)). To overcome the long range interaction, fermions makes dynamical doublons, results in increase in average double occupancy, $d(t) = \frac{1}{L} \sum_{i=1}^L \langle n_{i\uparrow} n_{i\downarrow} \rangle$ with time (Fig.3(b)). For larger value of V , due to formation of more doublons, the spin degree of freedom suppressed with time, which leads to vanishing of spin imbalance, $I_S(t)$, and suppression of spin fluctuations (Fig.3(c)). Thus, we find that in presence of V , the long time dynamics is controlled by mainly charge excitations, and spin dynamics suppressed after intermediate time $t \gtrsim 40\hbar/J$, which is quite opposite to the case with $V = 0$. Interestingly, the short time $t \lesssim 10\hbar/J$ dynamics can be qualitatively explain by effective exchange constant between two fermions $J_{i,j}^{ef}$ (as explain in Appendix in case of $\Delta = 0$, $J_{i,j}^{ef} \sim 4J^2/(U - V)$). The exchange constant⁵³ increase with increase in V and leads to faster growth of spin fluctuation $F_S(t)$, and rapid decay of spin-imbalance $I_S(t)$ at $V = 4$, compare to $V = 0$ (the expression of $J_{i,j}^{ef}$, should be valid only for short time and small V ($U \gg V$)).

B. With Disorder

In this subsection we explore localization of charge and spin in presence of quasi-periodic potential. As discussed in the previous section, without disorder in case of CDW product state $|\uparrow\downarrow 0 \uparrow\downarrow 0 \uparrow\downarrow 0 \uparrow\downarrow 0 \uparrow\downarrow \dots\rangle$ at $U \sim 2V$, the system relaxes with fastest rate and doublons are unstable. We first focus on localization at $U = 2V$, with initial CDW product state in presence of disorder Δ . We carried out the calculations with interaction parameters $U = 8.0$, $V = 4.0$, with system size $L = 12$ and varied the coefficient of Aubrey-Andre potential, Δ . To characterize the transition from delocalized phase to the MBL phase²⁴, first we probe the behavior of local observable charge imbalance $I(t)$ (in cold atom experiment $I(t)$ can be measured by using band mapping technique²⁶). As shown in Fig.4(a), in case of low disorder, the imbalance for the initial CDW state, relaxes quickly to zero. With increase in Δ , system starts localizing, and decay of $I(t)$ shows power law behavior with time (shown in Fig.4(a)). For strong disorder strength, $I(t)$, saturates to a constant value with time, indicates strong localization of particles. To measure the transition point from delocalized to MBL phase, with increase in disorder strength, we have

extracted the relaxation exponent²⁶ α , by power law fitting to the decay of $I(t) \sim t^{-\alpha}$ (between 10t to 100t). Fig.4(b) shows the disorder average relaxation exponent α , with disorder strength Δ , here α is averaged over eight to nine different values of the phase factor ϕ , for each Δ of the disorder potential. The exponent α monotonically decreases with increase in Δ and approaches to zero in MBL phase⁵⁴. As shown Fig.4(b), α approaches to zero at $\Delta \sim 6.0 \pm 1$, indicate transition from delocalized to MBL phase in the system for interaction parameter $U = 8$, $V = 4$.

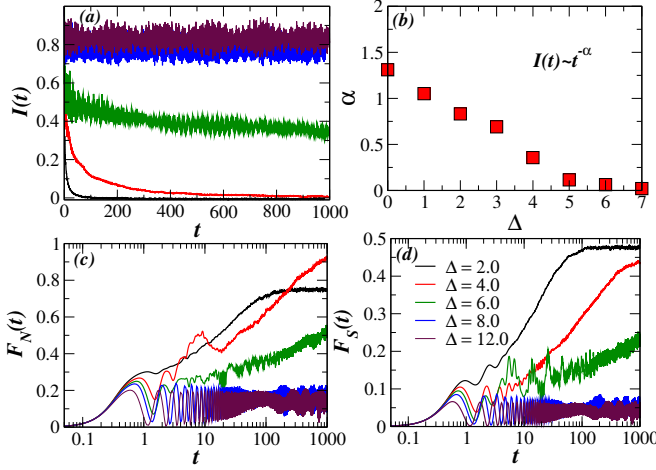


FIG. 4. (a) Charge imbalance $I(t)$, (b) disorder average exponent α of imbalance decay, (c) bipartite charge-fluctuation $F_N(t)$, (d) bipartite spin-fluctuation $F_S(t)$ with time t (in units of \hbar/J), at $V = 4$, $U = 8$ and for different values of Δ .

For many body localized state, particle and spin transport are forbidden, we analyze this phenomenon by observing the dynamics of charge $F_N(t)$ and spin $F_S(t)$ fluctuations. As shown in the Fig.4, for lower values of Δ , spin and charge fluctuations grows rapidly with time, indicates strong delocalization of charge and spin degree of freedom in the system. For lower values of disorder strength, doublons can break into single fermions (at $U = 2V$), which gives rise to enhance in charge $F_N(t)$ and spin $F_S(t)$ fluctuations in the system. Interestingly, near the phase boundary of delocalized to localized transition ($\Delta \sim 6.0$), charge $F_N(t)$ and spin-fluctuation, $F_S(t)$, grows slowly with time, indicate sub-diffusive transport of charge and spin degree of freedom^{46,48}. This slowdown of dynamics near the MBL-transition point, have recently been observed in ultra cold experiment with fermions subjected to quasiperiodic potential²⁶ For large values of disorder doublons are quite stable and localize; they do not breaks into single particles, which seizes the spin-fluctuation and charge-fluctuation in the system. We find that for large values of $\Delta \gtrsim 6.0$ both spin and charge fluctuation show oscillation around a small fixed value without increase in magnitude with time, which clearly indicates the absence of charge and spin transport in the system.

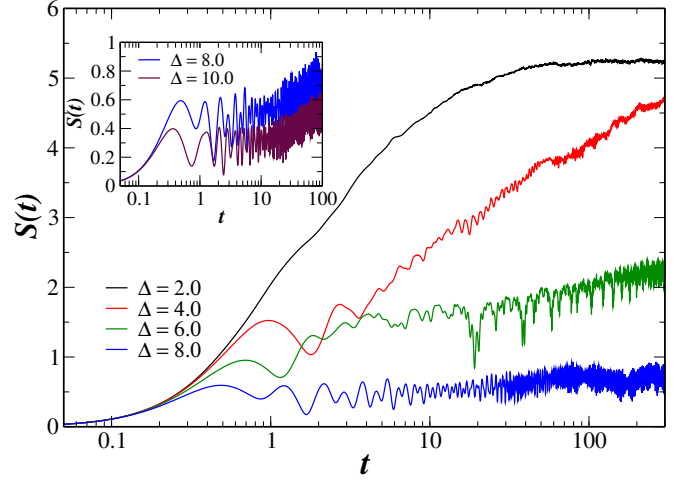


FIG. 5. Entanglement entropy $S(t)$, with time, t (in units of \hbar/J), at $U = 8$, $V = 4$, and for different values of Δ . Inset: entanglement entropy $S(t)$ for larger values of $\Delta = 8.0$ and 10

The dynamical entanglement entropy is one of the hall mark to characterize the MBL phase in the system. As shown in Fig.5, for lower values of Δ entanglement entropy, $S(t)$ (for $L = 10$) grows rapidly with time. Near the phase transition, the entanglement entropy grows in power law with time. This is due to the slow transport of particles and dephasing mechanism⁴⁶. For large values of $\Delta > 6.0$, $S(t)$ grows nearly logarithmic with time. The rate of the growth in entanglement entropy further slows down with increase in the strength of disorder strength, Δ (shown in the inset of Fig.5). After time $t \gtrsim 100$, entanglement entropy, $S(t)$, saturates due to the finite size of the system. The slow growth of entanglement, $S(t)$, for $\Delta \gtrsim 6.0$ along with frozen charge and spin fluctuations indicates appearance of MBL-phase in the system. This entanglement growth with time is solely due to the dephasing mechanism; as charge and spin transport get frozen but quantum correlation between distant sites can still evolve with time^{52,55}.

Next we focus on effect of long range interactions V , on spin degree of freedom, in presence of large disorder ($\Delta = 16$) and onsite-interaction ($U = 8$). We started the time evolution with Neel state $|\uparrow, \downarrow, \uparrow, \downarrow, \uparrow, \downarrow, \uparrow, \downarrow, \uparrow, \downarrow, \dots\rangle$, which corresponds to the almost middle part of the spectrum of Hamiltonian. In this limit of disorder strength, charge degree of freedom almost freezes, but spin excitation can propagate into the system by virtual hopping processes between different sites³⁵. With these virtual particle hopping, one can derive an effective spin model (with effective exchange constant $J_{i,j}^{ef}$), where the spins at different sites interact through the exchange mechanism^{33,35}. As shown in Fig.6, for $V = 0$, spin fluctuations $F_S(t)$, grows algebraically with time, due to the propagation of spin excitation in the system. With increase in V , the $J_{i,j}^{ef}$ get reduced (expression of $J_{i,j}^{ef}$ between two fermions is shown in Appendix) and leads

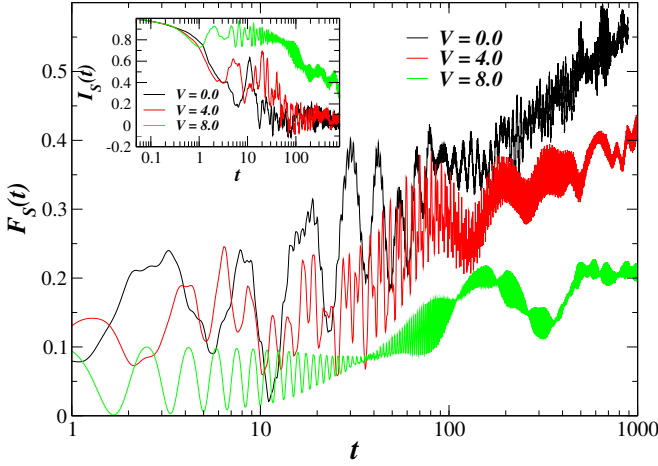


FIG. 6. Bipartite spin-fluctuation $F_S(t)$ with time, Inset: decay of spin imbalance $I_S(t)$ with time, t (in units of \hbar/J), at $U = 8$, $\Delta = 16$, $L = 12$ and different values of V .

to the suppression of propagation of spin excitation in the system. For $V = 8$ and $U = 8$, spin-fluctuation, $F_S(t)$, becomes almost constant after intermediate time, as there is almost no transport of spin degree of freedom. In the inset of Fig.6, we show the behavior of spin imbalance $I_S(t)$, for $V = 0$ and $V = 4$, $I_S(t)$ decay rapidly and oscillate around zero after time $t \gtrsim 100\hbar/J$, while for $V = 8$, $I_S(t)$ decay very slowly with time, indicates localization of spin degree of freedom. In fact, we find this behavior of localization of spin, holds at $U = V$ (for $V = 4$, $U = 4$ shown in the Appendix Fig.9), and qualitatively explain by the vanishing of effective exchange interaction $J_{i,j}^{ef}$ at $U = V$. In fact, we find that lower the value of interaction strength $U = V$, stronger the localization of spin degree of freedom.

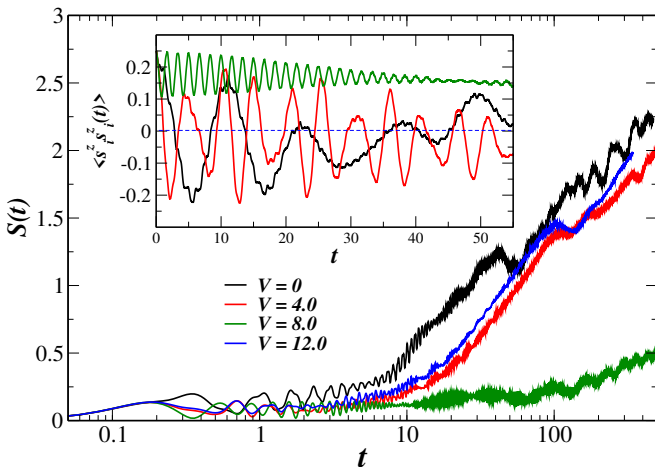


FIG. 7. Entanglement entropy $S(t)$ with time, Inset: spin auto-correlation function for site index $i = 6$ with time, t (in units of \hbar/J), at $U = 8$, $\Delta = 16$ and for different values of V .

To get more insight, we have also calculated entangle-

ment entropy $S(t)$, for $L = 10$, $U = 8$, $\Delta = 16$ and with varying long-range interaction V . As shown in Fig.7, for $V = 8$, entanglement entropy $S(t)$, grows nearly logarithmically, indicating presence of MBL-phase in the system. Whereas for $V = 0, 4$ and 12 , $S(t)$, grows rapidly with time, due to delocalization of spin-degree of freedom in the system. Interestingly, the rate of growth of entanglement entropy $S(t)$, with time not always decrease with increase in V . For $V = 12$, $S(t)$ grow rapidly with time (very similar to $S(t)$ at $V = 4$), which can roughly explained by increase in magnitude of the effective exchange constant $J_{i,j}^{ef}$, for $V > 8.0$ (see Appendix). In the inset of Fig.7, we show plot of spin auto-correlation $\langle s_i^z s_i^z(t) \rangle = \langle \psi(0) | s_{L/2}^z s_{L/2}^z(t) | \psi(0) \rangle$, with respect to initial Neel state and for site index $i = 6$. The spin auto-correlation function is also a local observable and represent local spin imbalance⁵⁴. For $V = 0$ and $V = 4$, $\langle s_i^z s_i^z(t) \rangle$ shows oscillation around zero and the amplitude of oscillation slowly reduces with time, indicating delocalization of spin-degree of freedom. On the contrary, for $V = 8$, $\langle s_i^z s_i^z(t) \rangle$, decay very slowly, indicates preservation of memory of the initial Neel state and localization of the spin degree of freedom.

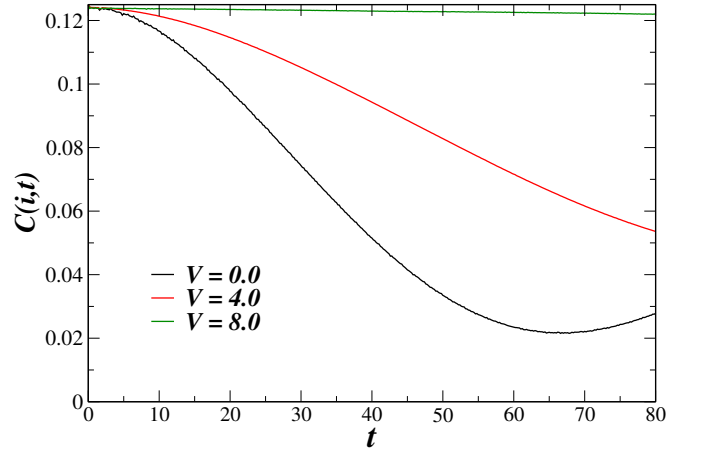


FIG. 8. Return probability $C(i, t)$ for site index $i = 4$ with time t (in units of \hbar/J), at $U = 8$, $\Delta = 16$ and for different values of V .

Thus far we have discussed the non-equilibrium dynamics for quantum quench starting with initial highly excited product states. To see the extent of localization of spin degree of freedom in the full energy-spectrum, we have calculated return probability⁵⁶, by full diagonalization of the system Hamiltonian for $L = 8$, $U = 8$, $\Delta = 16$ and different values of V .

$$C(i, t) = \frac{1}{D} \sum_n \langle \psi_n | s_i^z s_i^z(t) | \psi_n \rangle$$

$$= \frac{1}{D} \sum_{m,n} \exp(-it(E_n - E_m)) |\langle \psi_n | s_i^z | \psi_m \rangle|^2 \quad (2)$$

As we shown in Fig.8, the return probability $C(i=4, t)$, for $V = 0$ decay rapidly and oscillate to a smaller value

(oscillation may be due to finite size effect for $L = 8$), indicates delocalization of spin degree of freedom over large fraction of energy spectrum. For $V = 4$, $C(i = 4, t)$ decay algebraically and hinting at the reduction of delocalization of spin degree of freedom in the energy spectrum. On the otherhand, for $V = 8$, $C(i=4, t)$ almost constant with time, give signature of localization of spin degree of freedom over full energy spectrum.

IV. CONCLUSION

In conclusion, we have studied the localization of charge and spin degrees of freedom in dipolar fermions, in presence of quasiperiodic potential, by taking initial product states with doublons and a Neel state. In case of product state with doublons, without disorder, doublons breaks at $U \sim 2V$, and leads to delocalization charge and spin degree of freedom, while for larger values of onsite interactions, doublons remains intact and system become localized (note, even without disorder). In presence of quasiperiodic potential, we are able to locate the transition point, for transition from delocalized phase to localized MBL-phase, by estimation of relaxation exponent. We find for large disorder, spin and charge fluctuations freeze after short time, whereas, entanglement entropy increase slowly with time, which give clear signature of MBL phase in dipolar system even in presence of strong interactions and $SU(2)$ symmetry. In case of Neel state, we find in clean system spin degree of freedom delocalizes quickly, while with increase in long-range interactions, we observed formation of doublons and enhancement in charge fluctuations. On the otherhand, at large disorder and onsite interaction, charge degree of freedom localized, while spin show diffusive behavior. Interestingly, we find the localization of spin degree of freedom (even in presence of $SU(2)$ symmetry) when the strength of onsite and long range interactions are nearly same. The localization of spin degree of freedom, in presence of long-range interaction, is due to the reduction of effective exchange interactions. We demonstrate that in presence of large disorder, the localization of spin exists even in full energy-spectrum, when onsite and long-range interactions are similar in strength. The localization of spin and charge degree of freedom, with logarithmically increase in entanglement entropy, give possibility of existence of full-MBL phase in the system without breaking spin $SU(2)$ symmetry. Although, we have studied the dynamics at long enough time, but there is also possibility that for very large system and in longer time scale, system may have density and spin fluctuation due to strong long range and onsite interactions, which may leads to destruction of MBL phase.

V. ACKNOWLEDGMENTS

We thank Prof. Guillaume Roux and Dr. Eoin Quinn for useful discussions. We also thank LPTMS-University of Paris-Sud, for cluster facilities. S.K.P. acknowledges DST, SERB, JCBose Fellowship, Govt. of India for financial support.

VI. APPENDIX

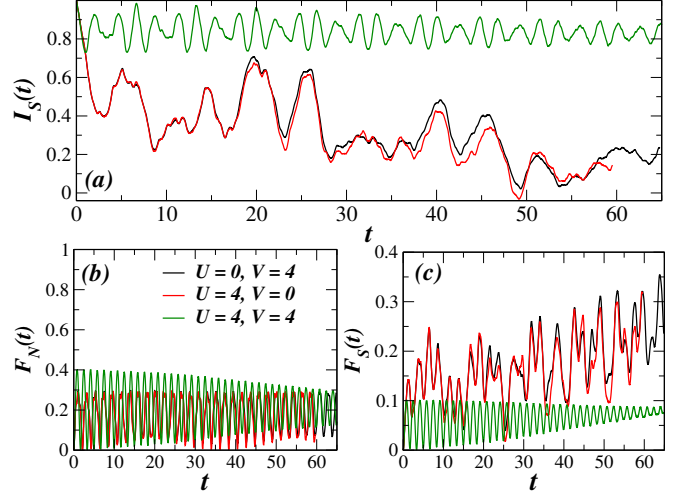


FIG. 9. (a) Spin imbalance $I_S(t)$, (b) bipartite charge-fluctuation $F_N(t)$ (c) bipartite spin-fluctuation $F_S(t)$, with time t (in units of \hbar/J), at $\Delta = 16$, $L = 12$ and for different values of U and V .

To get the insight in to the physical picture of localization of spin degree of freedom, we consider fermions interacting with onsite U and nearest-neighbor interactions V , in presence of large disorder strength Δ and system initialize in Neel state $|\uparrow, \downarrow, \uparrow, \downarrow, \uparrow, \downarrow, \uparrow, \downarrow, \dots\rangle$. In the limit of large disorder strength, charge degree of freedom localizes, but spin can interact through exchange mechanism. The exchange occurs from virtual hopping of an particle with spin \uparrow to a neighboring site with spin \downarrow or vice versa. In the limit of small interaction ($U, V \ll \Delta$), the dynamics of spin-degree of freedom can be described by Heisenberg model³⁵ $H_{spin} \sim \sum_{\langle i,j \rangle} J_{i,j}^{ef} S_i \cdot S_j$. The coupling strength $J_{i,j}^{ef}$ between two neighboring spin, can be found in the second order term of the perturbation expansion in hopping amplitude⁵⁷ J . Here starting with only two fermions $|\uparrow, \downarrow\rangle$ with opposite spins, and using canonical transformation of H :

$$\tilde{H} = \exp(iS\lambda)H \exp(-i\lambda S) \quad (3)$$

Writing, $H = H_D + \lambda H_J$ in the basis ($|\uparrow, \downarrow\rangle, |\downarrow, \uparrow\rangle, |\uparrow\uparrow, 0\rangle, |0, \uparrow\downarrow\rangle$) where the diagonal part of Hamiltonian ma-

trix:

$$H_D = \begin{pmatrix} \epsilon_1 + \epsilon_2 & 0 & 0 & 0 \\ 0 & \epsilon_1 + \epsilon_2 & 0 & 0 \\ 0 & 0 & 2\epsilon_1 + U - V & 0 \\ 0 & 0 & 0 & 2\epsilon_2 + U - V \end{pmatrix}$$

And the hopping term of Hamiltonian matrix:

$$H_J = \begin{pmatrix} 0 & 0 & -J & -J \\ 0 & 0 & J & J \\ -J & J & 0 & 0 \\ -J & J & 0 & 0 \end{pmatrix}$$

To get the hermitian S matrix, we used the condition $H_J + i[S, H_D] = 0$, which results in vanishing of first order term in hopping.

$$S = i \begin{pmatrix} 0 & 0 & -\frac{J}{A} & -\frac{J}{B} \\ 0 & 0 & \frac{J}{A} & \frac{J}{B} \\ \frac{J}{A} & -\frac{J}{A} & 0 & 0 \\ \frac{J}{B} & -\frac{J}{B} & 0 & 0 \end{pmatrix}$$

Where $A = (\epsilon_1 - \epsilon_2) + (U - V)$ and $B = (\epsilon_2 - \epsilon_1) + (U - V)$. After substituting the S matrix in the second order term of the perturbation expansion in hopping amplitude J/Δ and projecting into the subspace ($|\uparrow, \downarrow\rangle, |\downarrow, \uparrow\rangle$), we obtain the Heisenberg Hamiltonian $H = J_{i,j}^{ef} S_i \cdot S_j$ for two spin with exchange constant:

$$J_{i,j}^{ef} = -\frac{4J^2(U - V)}{(\epsilon_i - \epsilon_j)^2 - (U - V)^2} \quad (4)$$

we assume $\Delta > 12$ and $\epsilon_i = \Delta \cos(2\pi\beta i)$. The form of the exchange $J_{i,j}^{ef}$ able to explain qualitatively, the behavior of spin dynamics in presence of large disorder. As shown in Fig.9, for $U = 0, V = 4$ and $U = 4, V = 0$ the dynamics is quite similar upto intermediate time, as magnitude of $|J_{i,j}^{ef}|$ is same for these two value of interaction parameters (U and V). The spin-imbalance $I_S(t)$, slowly decay with time and approaches to zero (Fig.9(a)). The spin-fluctuations $F_S(t)$, also grows slowly, and shows global transport of spin fluctuations (Fig.9(c)). Whereas for $U = 4, V = 4$, the effective exchange $J_{i,j}^{ef}$ reduce to zero, the spin-imbalance, $I_S(t)$ remains close to initial values (Fig.9(a)) and spin-fluctuation $F_S(t)$, shows oscillations

around a fixed value (Fig.9(c)), indicate localization of spin degree of freedom. On the otherhand the charge fluctuation $F_N(t)$ always oscillates around a fixed values (Fig.9(b)) for all values of interaction parameters (U and V), conforms localization of charge degree of freedom for $\Delta = 16$.

To see the finite size effect we have also check the time evolution for larger system size ($L=24$), using matrix product operators (MPO) and matrix product state (MPS), based on ITensor library³⁸. For simplicity we consider only nearest-neighbor V terms along with on-site interaction U . In Fig.10, we have shown the plot of local spin imbalance ($I_s(t) = s_i^z - s_{i+1}^z$, $i=L/2$) and entanglement entropy $S(t)$, for $U = 8$, $\Delta = 16$ and different values of V . We find that, the decay of spin imbalance consistence with small system size, for the different values of V . For $V = 0$, $I_s(t)$, decay faster with time, while $V = 8$, it revive to same initial value with time (Fig.10(a)). The entanglement entropy, for $V = 0$ increases linearly with faster rate compare to $V = 4$ with time. On the otherhand, for $V = 8$, entanglement grows almost logarithmically with time (Fig.10(b)).

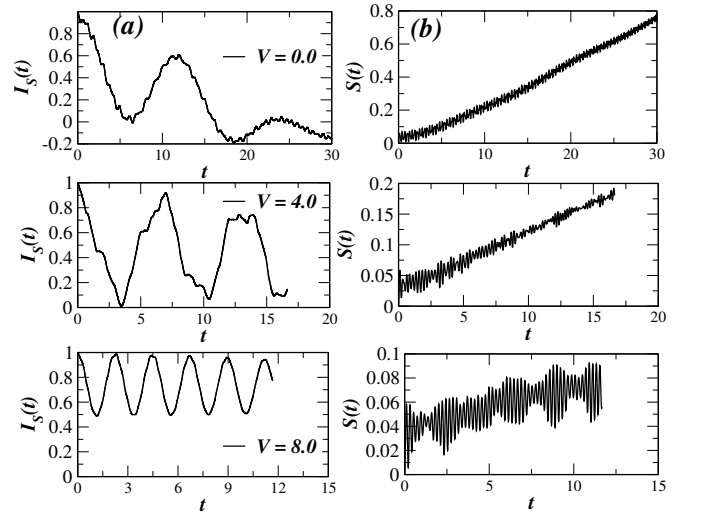


FIG. 10. In column (a), spin imbalance $I_S(t)$, (b) entanglement entropy $S(t)$, with time t (in units of \hbar/J), at $\Delta = 16$, $U = 8$, $L = 24$ and for different values of V .

- ¹ J. Eiders, M. Friesdorf, C. Gogolin, Nature Physics, **11**, 124 (2015).
- ² E. Altman, arXiv:1512.00870 (2015)
- ³ T. Langen, R. Geiger, and J. Schmiedmayer, Ann. Rev. Condens. Matter Phys. **6**, 201 (2015).
- ⁴ M. Greiner, O. Mandel, T. W. Hänsch, and I. Bloch, Nature, **419**, 51 (2002).
- ⁵ J. M. Deutsch, Phys. Rev. A, **43**, 2046 (1991)
- ⁶ M. Srednicki, Phys. Rev. E, **50**, 888 (1994)

- ⁷ D. A. Huse, Physics, **9**, 76 (2016)
- ⁸ T. Kinoshita, T. Wenger and D. S. Weiss, Nature (London), **440**, 900 (2006)
- ⁹ P. W. Anderson, Phys. Rev. **109**, 1492 (1958)
- ¹⁰ L. Sapienza, H. Thyrestrup, S. Stobbe, P. D. Garcia, S. Smolka, P. Lodah Science **327**, 1352 (2010)
- ¹¹ D.M. Basko, I.L. Aleiner, and B.L. Altshuler, Ann. Phys. (N.Y.) **321**, 1126 (2006)
- ¹² I.V. Gornyi, A.D. Mirlin, and D.G. Polyakov, Phys. Rev.

- Lett. **95**, 206603 (2005)
- ¹³ V. Oganesyan and D.A. Huse, Phys. Rev. B **75**, 155111 (2007)
 - ¹⁴ A. Pal and D.A. Huse, Phys. Rev. B **82**, 174411 (2010)
 - ¹⁵ R. Nandkishore and D. A. Huse, Annu. Rev. Condens. Matter Phys. **6**, 15 (2015)
 - ¹⁶ B. Bauer and C. Nayak, J. Stat. Mech., P09005 (2013)
 - ¹⁷ M. Serbyn, Z. Papic, and D. A. Abanin, Phys. Rev. Lett. **111**, 127201 (2013)
 - ¹⁸ D. A. Huse, R. Nandkishore, and V. Oganesyan, Phys. Rev. B **90**, 174202 (2014)
 - ¹⁹ M. Serbyn, Z. Papic, and D. A. Abanin, Phys. Rev. B **90**, 174302 (2014)
 - ²⁰ V. Ros and M. Muller, Phys. Rev. Lett. **118**, 237202 (2017)
 - ²¹ H. Kim and D. A. Huse, Phys. Rev. Lett. **111**, 127205 (2013)
 - ²² J. H. Bardarson, F. Pollmann, and J. E. Moore, Phys. Rev. Lett. **109**, 017202 (2012)
 - ²³ M. Serbyn, Z. Papic, and D. A. Abanin, Phys. Rev. Lett. **110**, 260601 (2013)
 - ²⁴ M. Schreiber, S. S. Hodgman, P. Bordia, H. P. Luschen, M. H. Fischer, R. Vosk, E. Altman, U. Schneider, I. Bloch, Science **349**, 842 (2015)
 - ²⁵ P. Bordia, H. P. Luschen, S. S. Hodgman, M. Schreiber, I. Bloch, U. Schneider, Phys. Rev. Lett. **116**, 140401 (2016)
 - ²⁶ H. P. Luschen, P. Bordia, S. Scherg, F. Alet, E. Altman, U. Schneider, I. Bloch, Phys. Rev. Lett. **119**, 260401 (2017)
 - ²⁷ J. Smith, A. Lee, P. Richerme, B. Neyenhuis, P. W. Hess, P. Hauke, M. Heyl, D. A. Huse, and C. Monroe, Nature Physics **12**, 907 (2016)
 - ²⁸ I. V. Protopopov, W. W. Ho, D. A. Abanin, Phys. Rev. B **96**, 041122 (2017)
 - ²⁹ A. C. Potter, R. Vasseur, Phys. Rev. B **94**, 224206 (2016)
 - ³⁰ A. Prakash, S. Ganeshan, L. Fidkowski, and Tzu-Chieh Wei, Phys. Rev. B **96**, 165136 (2017)
 - ³¹ P. Prelovsek, O. S. Barisic, and M. Znidaric, Phys. Rev. B **94**, 241104(R) (2016)
 - ³² J. Zakrzewski and D. Delande, Phys. Rev. B **98**, 014203 (2018)
 - ³³ M. Kozarzewski, P. Prelovsek, and M. Mierzejewski, Phys. Rev. Lett. **120**, 246602 (2018)
 - ³⁴ M. Sroda, P. Prelovek, and M. Mierzejewski, Phys. Rev. B **99**, 121110(R) (2019)
 - ³⁵ I. V. Protopopov and D. A. Abanin, Phys. Rev. B **99**, 115111 (2019)
 - ³⁶ K.-K. Ni, S. Ospelkaus, M. H. G. de Miranda, A. Pe'er, B. Neyenhuis, J. J. Zirbel, S. Kotochigova, P. S. Julienne, D. S. Jin, J. Ye, Science **322**, 231 (2008)
 - ³⁷ C. Wu, J. W. Park, P. Ahmadi, S. Will, and M. W. Zwierlein, Phys. Rev. Lett. **109**, 085301 (2012)
 - ³⁸ ITensor, <http://itensor.org>,
 - ³⁹ T. Giamarchi, Quantum Physics in One Dimension (Clarendon Press, 2004)
 - ⁴⁰ J. R. Garrison, R. V. Mishmash, and M. P. A. Fisher, Phys. Rev. B **95**, 054204 (2017)
 - ⁴¹ G. I. Japaridze and A. P. Kampf, Phys. Rev. B **59**, 12822 (1999)
 - ⁴² M. Tezuka and A. M. Garcia-Garcia, Phys. Rev. A **85**, 031602(R) (2012)
 - ⁴³ Shi-Xin Zhang and H. Yao, Phys. Rev. Lett. **121**, 206601 (2018)
 - ⁴⁴ H. Mosadeq and R. Asgari, Phys. Rev. B **91**, 085126 (2015).
 - ⁴⁵ F. Hofmann and M. Potthoff, Phys. Rev. B **85**, 205127 (2012)
 - ⁴⁶ M. Serbyn, Z. Papic, and D. A. Abanin, Phys. Rev X **5**, 041047 (2015)
 - ⁴⁷ H. Francis Song, S. Rachel, C. Flindt, I. Klich, N. Laflorencie, and K. Le Hur, Phys. Rev. B **85**, 035409 (2012)
 - ⁴⁸ R. Singh, J. H. Bardarson, F. Pollmann New J. Phys. **18**, 023046 (2016)
 - ⁴⁹ T. Enss and J. Sirker, New J. Phys. **14**, 023008 (2012)
 - ⁵⁰ A. Bauer, F. Dorfner, and F. Heidrich-Meisner, Phys. Rev. A **91**, 053628 (2015).
 - ⁵¹ V. Ros and M. Muller, Phys. Rev. Lett. **118**, 237202 (2017)
 - ⁵² F. Iemini, A. Russomanno, D. Rossini, A. Scardicchio, and R. Fazio, Phys. Rev. B **94**, 214206 (2016)
 - ⁵³ R. Eder, J. van den Brink, and G. A. Sawatzky, Phys. Rev. B **54**, R732(R) (1996)
 - ⁵⁴ D. J. Luitz, N. Laflorencie, and F. Alet, Phys. Rev. B **93**, 060201(R) (2016)
 - ⁵⁵ M. Pino, Phys. Rev. B **90**, 174204 (2014)
 - ⁵⁶ R. Modak and S. Mukerjee, Phys. Rev. Lett. **115**, 230401 (2015)
 - ⁵⁷ T. Barthel, C. Kasztelan, I. P. McCulloch, and U. Schollwock, Phys. Rev. A **79**, 053627 (2009)